The potential of scintillator-based photon counting detectors
Evaluation using Monte Carlo simulations

Hsieh, Scott S.; Taguchi, Katsuyuki; Goorden, Marlies C.; Schaart, Dennis R.

DOI
10.1117/12.3045837

Publication date
2025

Document Version
Final published version

Published in
Medical Imaging 2025

The potential of scintillator-based photon counting detectors: evaluation using Monte Carlo simulations

Scott S. Hsieh[a], Katsuyuki Taguchi [b], Marlies C. Goorden[c], Dennis R. Schaart[c],
[a]Dept. of Radiology, Mayo Clinic, Rochester, MN, USA 55902;
[b]Dept. of Radiology, Johns Hopkins University, Baltimore, MD, USA 21218;
[c]Dept. of Radiation Science and Technology, Delft University of Technology, Delft, Netherlands

ABSTRACT

Direct conversion photon counting detectors (PCDs) using CdTe, CZT, or Si for the sensor material are being investigated and manufactured. Indirect conversion, scintillator-based PCDs have historically thought to be too slow for the high flux requirements of diagnostic CT. Recent scintillators investigated for e.g. PET applications are very fast and inspire us to rethink this paradigm. We evaluate the potential of a $LaBr_3$:Ce PCD using Monte Carlo simulations. We compared a CdTe PCD and a $LaBr_3$:Ce PCD, assuming a pixel density of 9 pixels/mm^2 in each case and a surrounding 2D anti-scatter grid. A 1x1 mm^2 area was illuminated by flat field X-rays and the lower bound on the noise for varying contrast types and material decomposition scenarios was calculated. For conventional imaging without material decomposition, the $LaBr_3$:Ce PCD performed worse than CdTe because of the need to wrap pixels in reflector, which reduces geometric efficiency. For water-bone material decomposition, the two PCDs performed similarly with our assumptions on pulse shape and PCD geometry. For three-material decomposition with a K-edge imaging agent, $LaBr_3$:Ce reduced variance by about 35% because of the elimination of charge sharing that is present in CdTe. These results motivate further exploration of scintillator-based PCDs as an alternative to direct conversion PCDs, especially with future K-edge imaging agents.

Keywords: photon counting detectors, dual energy imaging, scintillators

1. INTRODUCTION

Photon counting detectors (PCDs) are the latest major advance in x-ray computed tomography (CT) (1, 2). Two PCD CT scanners have been approved by regulatory authorities in the United States, and several other models have entered human trials. These scanners all feature double the spatial resolution compared to conventional CT and also provide the ability to retrospectively access spectral data (3). All PCD CT scanners under active development use a direct conversion sensor, either cadmium-based (CdTe/CZT) or silicon. These materials are “direct conversion” because the incident X-rays are converted directly into electrons and holes. Both of these sensor materials have relatively poor signal-to-noise ratio (SNR) of spectral data: CdTe/CZT is corrupted by charge sharing, whereas silicon must deal with a high prevalence of Compton events that provide relatively little spectral signal.

Indirect conversion sensors are also available that use visible light as an intermediate step. These PCDs consist of a fast scintillator, such as LaBr3:Ce, coupled to a fast photosensor, such as a silicon photomultiplier tube (SiPM). LaBr3:Ce is a very fast scintillator that has amongst others been investigated for time-of-flight PET, having a 16 ns scintillation decay time constant (4, 5). These fast speeds make scintillator-based clinical PCD CT a possibility.

A major difference of indirect and direct conversion PCDs is that in indirect conversion PCDs each scintillator pixel must be wrapped with a light reflector (Fig. 1). This is both a positive and a negative: the positive is that these reflectors efficiently isolate each pixel from its neighbors, so that charge sharing is minimized. (Light leakage does occur, but it is not very spatially-dependent, and the amount of leakage signal can be kept underneath the first energy threshold.) The negative is that this reduces the fill factor of the PCD, causing some X-ray photons to remain undetected and hence reducing quantum efficiency for non-spectral tasks.

Construction and evaluation of a scintillator-based PCD is a major undertaking. The purpose of this work is to predict the effectiveness of such a PCD using Monte Carlo simulations to determine if construction of a physical prototype is warranted.

Medical Imaging 2025: Physics of Medical Imaging, edited by John M. Sabol, Ke Li, Shiva Abbaszadeh, Proc. of SPIE Vol. 13405, 1340537 · © 2025 SPIE
1605-7422 · doi: 10.1117/12.3045837

2. METHODS

2.1 Monte Carlo simulator

We extended the PcTK Monte Carlo simulation program, which cascaded the following processes: (1) photon generation following Poisson statistics, (2) energy deposition based on selection of a uniform random incident location, (3) pulse train generation with electronic noise, and finally (4) digital counting following crossing of energy thresholds of a bank of comparators. We modeled a 3×3 block of pixels surrounded by anti-scatter grids (Fig. 1), which we assumed perfectly isolated the 3×3 pixels from other pixels, and assumed uniform radiation on the 3x3 block of pixels.

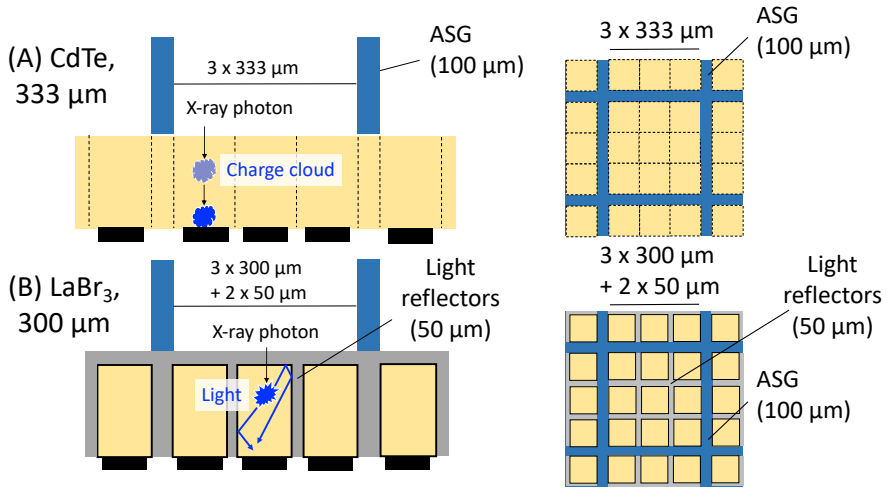

Figure 1. Side views and top views of CdTe PCD (A) and $LaBr_3$:*Ce* PCD (B) investigated in this study. ASG = anti-scatter grid. Used with permission from Reference (8).

2.2 Parameter selection

For the reference CdTe PCD, we assumed a pixel size of $(333\ \mu m)^2$, thickness of 2.0 mm, Gaussian charge cloud with a diameter of 72 µm full-width-at-half-maximum (FWHM) (7), pulse duration of 14 ns at FWHM, and electronic noise added to the pulse train. The energy deposition included temporal effects used in Ref (8).

For $LaBr_3$:Ce we assumed a pixel size of $(300\ \mu m)^2$, white reflector layer width of 50 µm between pixels (so that each 3x3 "macro-pixel" has a pitch of 1 mm, matched with CdTe), thickness of 3.0 mm, light leakage of 10% in total to 4 neighbor pixels, double-exponential shaped pulse duration of 26 ns at FWHM (4), and electronic noise added to the pulse train. These parameters were selected following recent experimental results in the literature, and we believe that they are an achievable target for a next-generation prototype module. The energy deposition step was generated by GEANT4, from which we created a library of interactions that was randomly sampled in this simulation.

For each PCD, we considered event detection using either threshold-subtract (counting up-crossings for each threshold energy and subtracting threshold data to produce energy binned data) or direct binning (which seeks to select the maximum energy only of each pulse and place the event directly into an energy bin, which improves performance at high pileup) (1, 6). The detection efficiency of 3-mm-thick $LaBr_3$:Ce was comparable to 2-mm-thick CdTe.

2.3 Evaluation methods

We assessed the recorded spectrum, counting capabilities, and spectral imaging task performances of both $LaBr_3$:Ce and CdTe. The following settings were used: flat-field irradiation from a 120 kVp spectrum with 2 mm aluminum and 10 cm water operated at tube current values of 20–1,000 mA. Threshold energies were set at [20, 45, 70, 95] keV. The outputs of 3×3 pixels were summed to create a macro-pixel (or super-pixel) output with $(1\ mm)^2$ aperture. We used 10,000 noise realizations for each tube current setting. Bootstrap resampling was performed to estimate standard deviation. Noise was assessed using the Cramér–Rao lower bound (CRLB) of the variance in several types of material decomposition tasks. The CRLB is used because there is not yet a consensus agreement on how material decomposition images should be produced from energy bin data. The CRLB describes the limiting noise behavior. In practice, it can usually be achieved

with the maximum likelihood estimator, but exceptions such as very low flux exist, and the maximum likelihood estimator may be too computationally slow to be used in many applications.

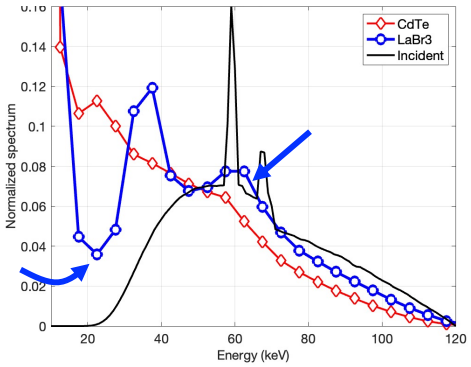

Figure 2. The incident spectrum, and the spectra recorded by CdTe PCD and $LaBr_3$:Ce PCD.

3. RESULTS

3.1 Spectrum

Figure 2 shows the incident and recorded spectra. It can be seen that the $LaBr_3$:Ce spectrum represented the incident spectrum more truthfully than the CdTe spectrum did, with a distinct bump near 60 keV where the characteristic x-rays of tungsten anode are present (blue arrow) and fewer counts for 15–25 keV (blue curved arrow). The peak at 35–40 keV reflected K-fluorescence x-rays of lanthanide. In contrast, the spectrum recorded by CdTe was distorted significantly even though the pixel size was larger (333 µm versus 300 µm). For both spectra, the increased counts below 15 keV (which may be due to noise, light leakage, or low-energy charge sharing) would not be detected in a typical PCD because it would be underneath the lowest energy threshold.

Figure 2 contrasts the mechanisms of spectral distortion present in direct and indirect conversion PCDs. CdTe is corrupted by charge sharing, creating a long tail of low-energy events. This dilutes spectral contrast and is known to increase variance in material decomposition images by more than a factor of three in prior simulation studies. $LaBr_3$:Ce, on the other hand, suffers from travel of characteristic x-ray photons to adjacent pixels. This is present in CdTe too, although the range of travel is less because of the lower energy of the characteristic x-ray. In $LaBr_3$:Ce this leads to corruption of the 35-40 keV window, where it may compete with low-energy primary photons. This suggests a few possible solutions: (1) the spectrum could be modified to reduce low-energy primary photons, by increasing the X-ray source kVp or by adding

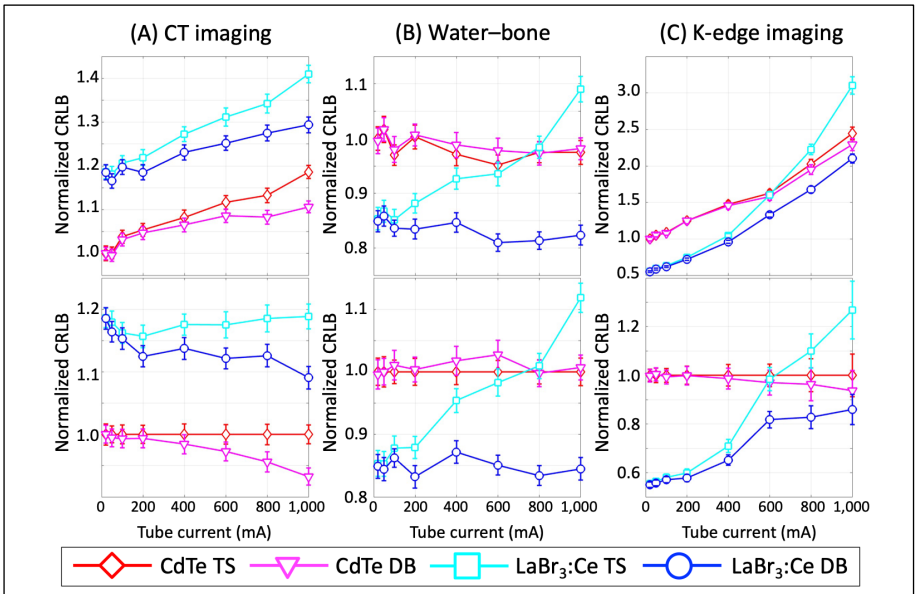

Figure 3. CRLB values for 3 spectral imaging tasks, normalized to CdTe TS at low tube current count. TS = threshold–subtract detection scheme; DB = direct energy binning. Normalized CRLBs for an ideal detector for the three tasks are (a) 0.79 for CT imaging, (b) 0.24 for water-bone, and (c) 0.13 for K-edge imaging. Used with permission from Reference (8).

filtration; (2) another scintillator could be used with lower energy characteristic X-rays; or (3) the detector circuitry could be modified to detect 35-40 keV photons and automatically combine them with a count in an adjacent pixel, if available. This modified circuitry would function as a charge summing circuit, but has the advantage that the characteristic X-ray energy is known a priori, and that charge summing would only occur when one event is 35-40 keV so that the pileup penalty from two independent photons is reduced.

3.2 Spectral imaging tasks

Normalized CRLB values are presented in Fig. 3. For conventional (non-spectral) imaging in Fig. 3A, we observed that (1) CRLB values increased almost monotonically with increasing tube current due to pulse pileup; (2) CRLBs of $LaBr_3$:Ce were about 20% higher than those of CdTe due to increased dead area as seen in Fig. 1; (3) DB outperformed TS, with the advantage increasing at higher mA.

The normalized CRLB values for the water–bone material decomposition are presented in Fig. 3(B). $LaBr_3$ when using direct binning performs better than CdTe across the entire operating range.

K-edge imaging CRLBs are presented in Fig. 3(C). Our observations are: (4) CRLB values increased almost monotonically with increasing tube current values due to pulse pileup; (5) CRLBs of $LaBr_3$:Ce were 30–40% lower than those of CdTe; and (6) for $LaBr_3$:Ce, DB provided significant advantage over TS at high mA. K-edge imaging was spectrally the most demanding imaging task among the three imaging tasks investigated. The spectral distortion of CdTe via charge sharing is particularly damaging for K-edge imaging, because photons above the K-edge could randomly be corrupted to be below the K-edge, which dilutes the spectral contrast. In comparison, the distortion of LaBr3:Ce is less disruptive: the majority of photons will be sampled at the correct energy.

4. CONCLUSIONS

We have studied the possible performance of a $LaBr_3$:Ce PCD module. The encapsulation of $LaBr_3$:Ce scintillator by reflectors allows it to have very good spectral performance with potential to be significantly better than CdTe PCD-CT for K-edge imaging applications, while the geometrical efficiency of $LaBr_3$:Ce will be worse than CdTe. The speed of this scintillator is now sufficient for many CT imaging tasks. We believe it is worth revisiting scintillator PCDs as a possible option for future PCD CT scanners.

REFERENCES

1. Taguchi K, Iwanczyk JS. Vision 20/20: Single photon counting x-ray detectors in medical imaging. Medical Physics. 2013;40(10):100901.
2. Taguchi K, Blevis I, Iniewski K. Spectral, Photon Counting Computed Tomography. Iniewski K, editor. New York: CRC Press. Taylor & Francis Group; 2020 July 15, 2020.
3. Hsieh SS, Leng S, Rajendran K, Tao S, McCollough CH. Photon Counting CT: Clinical Applications and Future Developments. IEEE Transactions on Radiation and Plasma Medical Sciences (published online, accessible on August 31, 2020 DOI:101109/TRPMS20203020212). 2020;5(4):441-52. doi: 10.1109/TRPMS.2020.3020212.
4. van der Sar SJ, Brunner SE, Schaart DR. Silicon photomultiplier-based scintillation detectors for photon-counting CT: A feasibility study. Medical Physics. 2021;48(10):6324-38. Epub 20210625. doi: https://doi.org/10.1002/mp.14886.
5. van der Sar SJ, Leibold D, Brunner SE, Schaart DR, editors. LaBr3: Ce and silicon photomultipliers: towards the optimal scintillating photon-counting detector. 7th International Conference on Image Formation in X-Ray Computed Tomography; 2022: SPIE.
6. Taguchi K, Hsieh SS. Direct energy binning for photon counting detectors: Simulation study. Medical Physics. 2024;51(1):70-9. doi: https://doi.org/10.1002/mp.16841.
7. Hsieh SS, Sjolin M. Digital count summing vs analog charge summing for photon counting detectors: A performance simulation study. Medical Physics. 2018;45(9):4085-93. doi: 10.1002/mp.13098.
8. Taguchi K, Iwanczyk JS. Assessment of multi-energy inter-pixel coincidence counters for photon-counting detectors at the presence of charge sharing and pulse pileup: A simulation study. Medical Physics. 2021;48(9):4909-25. doi: https://doi.org/10.1002/mp.15112.